



Design and optimization of a modular hydrogen-based integrated energy system to maximize revenue via nuclear-renewable sources

December 2024

Changing the World's Energy Future

Sadab Mahmud, Binaka Ponkiya, Sravya Katikanen, Srijana Pandey, Kranthikiran Mattimadugu, Zonggen Yi, Victor G Walker, Congjian Wang, Tyler L Westover, Michael Heben, Raghav Khanna, Ahmad Y. Javaid



DISCLAIMER

This information was prepared as an account of work sponsored by an agency of the U.S. Government. Neither the U.S. Government nor any agency thereof, nor any of their employees, makes any warranty, expressed or implied, or assumes any legal liability or responsibility for the accuracy, completeness, or usefulness, of any information, apparatus, product, or process disclosed, or represents that its use would not infringe privately owned rights. References herein to any specific commercial product, process, or service by trade name, trade mark, manufacturer, or otherwise, does not necessarily constitute or imply its endorsement, recommendation, or favoring by the U.S. Government or any agency thereof. The views and opinions of authors expressed herein do not necessarily state or reflect those of the U.S. Government or any agency thereof.

Design and optimization of a modular hydrogen-based integrated energy system to maximize revenue via nuclear-renewable sources

Sadab Mahmud, Binaka Ponkiya, Sravya Katikanen, Srijana Pandey, Kranthikiran Mattimadugu, Zonggen Yi, Victor G Walker, Congjian Wang, Tyler L Westover, Michael Heben, Raghav Khanna, Ahmad Y. Javaid

December 2024

**Idaho National Laboratory
Idaho Falls, Idaho 83415**

<http://www.inl.gov>

**Prepared for the
U.S. Department of Energy
Under DOE Idaho Operations Office
Contract DE-AC07-05ID14517**

Design and Optimization of a Modular Hydrogen-Based Integrated Energy System to Maximize Revenue via Nuclear-Renewable Sources

Sadab Mahmud^a, Binaka Ponkiya^a, Sravya Katikaneni^a, Srijana Pandey^a, Kranthikiran Mattimadugu^a, Zonggen Yi^b, Victor Walker^b, Congjian Wang^b, Tyler Westover^b, Ahmad Y Javaid^a, Michael Heben^a, Raghav Khanna^{a,**}

^aThe University of Toledo, Toledo, OH, USA

^bIdaho National Laboratory, Idaho Falls, ID, USA

Abstract

This paper demonstrates a novel modular distributed framework that uses optimal energy-dispatching strategies to enable greater flexibility and profitability in nuclear-renewable integrated energy systems (NR-IES). Hydrogen is used as a commodity in this framework since its production can improve grid stability and system operational flexibility, decarbonize heavy industry, and create an additional revenue stream for electricity generators, particularly nuclear power plants with high operational expenses. The proposed solution addresses the challenges associated with merging multiple software and services from various domains by using functional mock-up units (FMU) to co-simulate diverse subsystems designed in various platforms. The tightly coupled IES is optimized to maximize revenue by utilizing the deep reinforcement learning (DRL) technique to make smart dispatching decisions based on variable electricity prices and the availability of renewable energy. Proximal policy optimization (PPO) algorithm is used in training and testing the DRL agent. Over a period of 120 days, the proposed hydrogen-based IES framework showed about 10% revenue boost compared to a non-hydrogen generating baseline IES while also providing an easily-adoptable framework which can help to improve the flexibility of future generation nuclear power plants.

Keywords: Nuclear renewable integrated energy system, functional mock-up interface, co-simulation, deep reinforcement learning, hydrogen, control strategies, optimization.

1. Introduction

To address the global environmental challenges associated with climate change, a transition from fossil fuel-based to low-carbon energy sources, such as nuclear-derived power and renewable energy is needed [1], [2], [3]. Nuclear reactors provide 20 percent of the nation's power but have high operating costs and low revenue generating potential, particularly during times of low electricity prices. Due to the fact that they operate at baseload and have relatively low ramp rates (response times), most nuclear power plants are not readily capable of following the demand at the grid, thereby rendering them inflexible. Some nuclear plants can deliver power at 70% of their full capacity; however, this level is still too high to allow for profitability particularly when energy prices are depressed.

*Sadab Mahmud and Binaka Ponkiya contributed equally to this work.

**Corresponding author.

Email address: Raghav.Khanna@utoledo.edu (Raghav Khanna)

Wind and solar are sources of low-cost alternative energy [4] and are recognized as being renewable and sustainable in perpetuity. However, wind and solar energy are intermittent and vary widely according to geographical location and climatic circumstances. The tension between the high operating costs and inflexibility of nuclear power plants, in addition to the intermittency of renewable energy, requires that integrated energy ecosystems be implemented, with emphasis on profitability, sustainability, and flexibility.

Integrated nuclear-renewable energy systems are seen as a promising solution [5]. Such integrated energy systems (IES) are envisioned as a nuclear power plant coupled with renewable energy generation and industrial operations that can simultaneously address grid flexibility, global warming challenges, and revenue maximization [6], [7], [8]. Rather than investing in infrastructure expansion, combining diverse energy systems and running them within the same ecosystem can provide a more cost-effective and flexible solution for reliably fulfilling grid demand [9]. Implementing multi-input/multi-output IES can enable nuclear energy to support the production of additional commodities, such as hydrogen (H_2), while also providing power for the grid and complementing the expansion of variable renewable energy [10].

In recent years, the US Department of Energy, in addition to federal governments across the world, are recognizing the role that hydrogen must play in decarbonizing industries such as manufacturing, chemical fertilizer production, as well as long-haul transportation over land, sea, and air [11]. As an alternative energy carrier, hydrogen can interface with a variety of energy sources, namely fossil fuels, nuclear power, and renewables, for various applications [11], [12]. Due to its convenient long-term storage properties, it is seen as a secondary energy source that can play a crucial part in the transition to a low-carbon future. However, to reduce carbon emissions, hydrogen must be produced utilizing green energy sources like solar, wind, and nuclear energy [13], [14]. Incorporating hydrogen production and storage into a hybrid energy system complements the electric and natural gas grids to promote a smooth transition to a clean energy future [15]. Furthermore, as the scale of hydrogen production and utilization increases, it is expected that its production costs will decrease [16], and hydrogen will become more appealing. Thus, the production of hydrogen as a commodity in a nuclear-renewable-based integrated energy system has a wide range of practical applications while also offering an additional revenue stream.

The complexities of grid stability, the profitability of the hydrogen economy, and the intermittency of wind and solar power, combined with the inflexibility of nuclear power plants, can be understood and dealt with through modeling and simulation. Such simulations can be used to optimize and improve the performance of the envisioned IES [6], [17]. A challenging aspect of designing and simulating complex IES frameworks is the integration of the specialized subsystem models [18]. In recent years, significant research efforts have focused on combining two or more modeling platforms to incorporate characteristics of different domains utilizing cooperative simulation (co-simulation). Such co-simulation frameworks can provide modularity and excellent flexibility in the simulation of an IES. To support the development of co-simulation frameworks and methodologies, emerging technologies, such as the functional mock-up interface (FMI) implemented by a functional mock-up unit (FMU), can be utilized [19].

The operation of an IES, which includes multiple actors and assets, must be optimized to ensure maximum flexibility and profitability. If the renewable energy resource values can be predicted, mathematical programming can generate an accurate optimal energy management solution [20]. However, due to supply and demand variability, scheduling the renewable energy conversion is challenging. Some investigations employed deterministic optimization principles to address the unpredictable nature of renewable energy [21]. Nevertheless, applying deterministic principles to non-stationary systems cannot ensure optimal performance, and modifying variables may result in capital losses. Dynamic programming (DP) approach can be used to update the state-action pair at each step in time series decisions [22]. However, DP requires knowledge about the system’s transition probabilities over time. Additionally, systems with many states and actions suffer from the “curse of dimensionality.” Metaheuristic methods, such as particle swarm optimization (PSO) [23], are frequently employed for non-linear optimization. Yet, these strategies cannot ensure the global optimum. Furthermore, they cannot store optimization knowledge for a new assignment, resulting in low search efficiency. With the rapid advancement of artificial intelligence (AI) in recent years, more research has employed machine learning to optimize decision-making challenges in IES. The deep reinforcement learning (DRL) technique is a promising method for optimizing the dynamics associated with electricity pricing, energy generation, and consumption in energy management systems [24], [25].

This paper demonstrates a novel modular distributed framework that leverages DRL to optimize energy dispatching strategies, thereby enabling greater flexibility and profitability in nuclear-renewable integrated energy systems (NR-IES). The optimal dispatching strategies heavily rely on stochastic grid pricing. This paradigm of trading energy based on dynamic grid prices in order to increase revenue for energy providers while simultaneously reducing costs for consumers, particularly with an eye towards underserved areas, is known as *Transactive Energy* (TE) [26], and is gaining traction across the energy sector. By implementing the concepts of TE, this paper utilizes DRL to optimize the energy dispatching decisions in a flexible, profitable, and tightly-coupled framework by promoting hydrogen production during low energy prices and by prioritizing the integration of nuclear-derived power into the grid otherwise. Previous studies have demonstrated the superiority of DRL over conventional optimization techniques for obtaining optimal operation in energy management systems [17], [27]. In addition, the proposed DRL-based NR-IES framework circumvents the need for a complex mathematical optimization model. Furthermore, this work introduces easy integration and cooperative simulation of multiple subsystems via FMI and presents a use case for hydrogen to help maximize the overall IES revenue.

The contributions in this paper offer an adaptable and extensible framework and show how TE can be used to: (i) improve the profitability and flexibility of existing nuclear power plants; (ii) provide an easily adoptable framework to promote expansion of nuclear power, and guide future installations of small modular reactors (SMRs) within an IES; and (iii) decarbonize steel, glass, transportation, and other heavy industries with low-cost hydrogen production. The above-mentioned objectives are achieved through implementing a tightly coupled, high-fidelity, predictive IES framework in a novel co-simulation environment, as described by the following:

1. Development of a scalable computational framework to aid in the study of optimizing NR-IES operations utilizing DRL.
2. Demonstration of a modular NR-IES co-simulation framework architecture designed using various models developed in Python, Modelica, and Simulink platforms exported to FMU packages.
3. Management of a hydrogen-based NR-IES utilizing proximal policy optimization (PPO) [28], a DRL technique to make smart decisions and dispatching strategies based on varying electricity prices and renewable energy generation to attain higher revenues and flexibility.

Relative to previously reported frameworks that have also successfully improved the profitability and flexibility of NR-IES systems, a key contribution of this paper is the simplicity of the proposed framework, as well as its modularity, both of which allow it to be adopted fairly straightforwardly.

The remainder of this paper is structured as follows. Section 2 introduces the proposed framework design and details the modeling and simulation of the framework. The DRL computational methodology and discussion on the PPO algorithm used for optimization are provided in Section 3. Performance analysis of the NR-IES, including and excluding the hydrogen production in the framework, is detailed in Section 4. Finally, Section 5 concludes the paper and highlights the potential future work aspects.

2. Framework Design

The proposed integrated scheme is shown in Fig. 1. According to fluctuating grid pricing, various actors dispatch and receive energy. During periods of low demand, nuclear power is used to facilitate H₂ production via electrolysis.

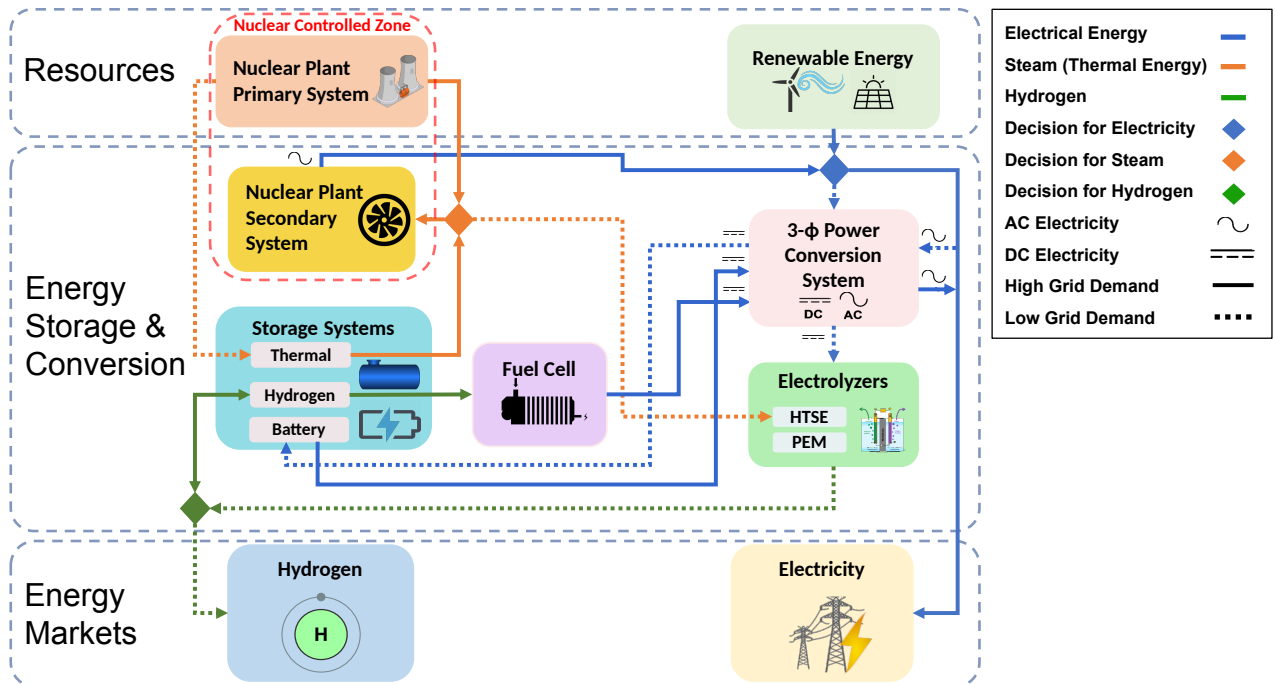


Figure 1: Energy flow diagram for NR-IES.

At times of high demand, H₂ production is ramped down, and nuclear-generated electricity is supplied to the grid. It should be noted that these actions are not mutually exclusive and can occur simultaneously. In Fig. 1, the dotted lines denote the actions that are more heavily weighted during times of low grid demand but still occur during times of high grid demand. Similarly, the actions represented by solid lines have a higher priority at high grid demand. For example, H₂ production is still ongoing and is supplied to the hydrogen market during high grid demand; but during low grid demand, the supply and production of hydrogen are prioritized and ramped up. Other assets, such as solar, wind, and additional energy storage systems, are used to support the grid according to its needs.

In [29], it was demonstrated that a single tool cannot always simulate all aspects of a complex system, whereas a group of interconnected tools gives additional modeling possibilities. Co-simulation frameworks enable the modeling and simulation of the numerous components of complex systems, taking advantage of the unique characteristics and features of each modeling tool. However, models developed in different platforms are not directly compatible with each other and require a unified framework that would enable the simulation of the entire system, such as the NR-IES proposed in this paper. Based on the FMI standard, modeling applications such as Dymola, Open Modelica, PyMT (Python Modeling Tool Kit), Simulink/MATLAB, etc., can produce C or binary code and a metadata file to represent a dynamic system component model and export it as an FMU integrated with a solver [19]. Additionally, such co-simulation frameworks allow the user to select from a variety of open-source models developed for a desired subsystem on any platform supporting the FMI standard.

Utilizing an FMI/FMU-based co-simulation framework, this work integrates platform-specific models through effective cross-domain scenario configuration. This study does not aim to develop a model-based method for optimizing the proposed NR-IES framework. Model-based optimization can deliver adequate performance if the underlying systems are accurately modeled, which requires considerable effort, especially for complex systems. However, the proposed framework is a combination of high-fidelity and generalized models wherein the core functionalities of high-level operation in each subsystem are considered and detailed in the following subsections, which is sufficient to validate the DRL-based method used to optimize the proposed NR-IES. Therefore, this work is able to achieve

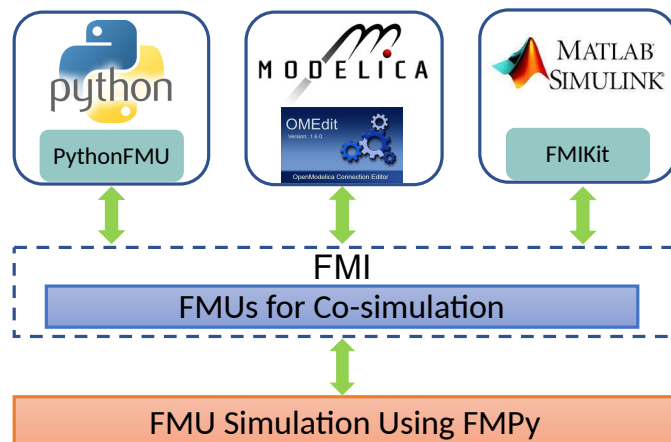


Figure 2: FMI/FMU framework.

good levels of fidelity, as reported in other works, but in a significantly simpler manner while allowing the NR-IES to demonstrate greater flexibility and profitability. The DRL-based optimization problem formulation for the proposed NR-IES is detailed in Section 3.1.

Fig. 2 summarizes the various tools used to export the FMUs of the models used in this paper. FMPy, an open-source Python library, is utilized to simulate the FMUs and produce results based on the varying state change [30]. The modeling and export of subsystems using three different tools, as shown in Fig. 2, along with the generation and pricing data used in the simulation of the proposed framework, are discussed below.

2.1. Python Models

The thermal energy storage (TES), polymer electrolyte membrane (PEM), and hydrogen energy storage (HES) subsystems are developed in Python programming language and exported to FMUs using PythonFMU [31]. While the FMUs exported using PythonFMU capture all of the modeling features, their performance remains stable and fast. The modeling of these Python-based subsystems is described as follows:

2.1.1. Thermal Energy Storage

Thermal energy can be stored by heating or cooling a storage medium. The stored thermal energy can be utilized for heating, cooling, and power production. By reducing fuel combustion requirements, the TES system lowers operating costs and environmental impacts. Additionally, it decreases thermal energy losses by holding surplus heat until it can be utilized. Within the NR-IES framework, the TES stores thermal energy produced by the nuclear plant primary system (NPPS). In the proposed framework, a capacity of 10000 MWh_{th} is considered as shown in Fig. 3, and the charge/discharge power is specified in MW_{th} . A thermal transfer loss of 1% is considered for this model, assuming some amount of loss due to energy exchange.

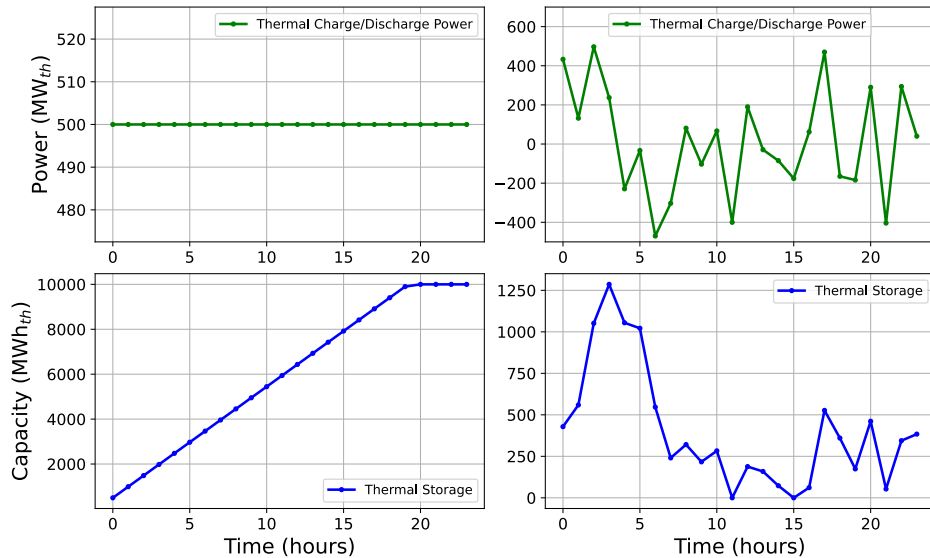


Figure 3: TES charging/discharging behavior for 24 hours.

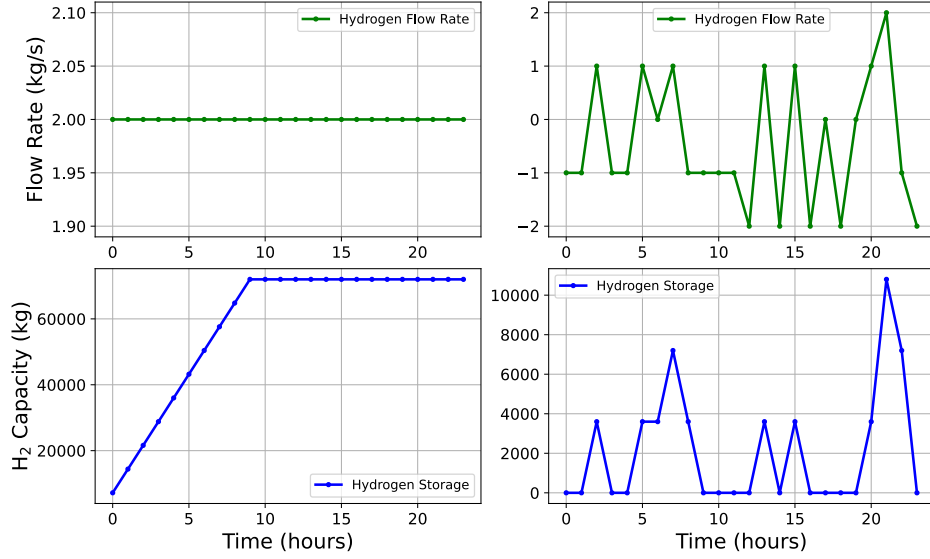


Figure 4: HES charging/discharging behavior for 24 hours.

Fig. 3 depicts the sample charging and discharging behavior of TES throughout a day. A positive power value is used for charging, and a negative value for discharging. The left column plots in Fig. 3 show that after 24 hours of charging at $500 \text{ MW}_{\text{th}}$, the TES will reach full capacity at 20th hour mark and remain constant if it is still getting charged. The right column plots in the figure depict the effect of stochastic charge and discharge power on TES and its behavior over time.

2.1.2. Hydrogen Energy Storage

The functionality of HES in the proposed framework is to store the hydrogen produced by the PEM and HTSE electrolyzers. This stored hydrogen can be used to meet demand when production falls short or supplied to fuel cells to generate electricity during high grid prices. The capacity taken into account for this model is 72000 kg. The operation of the HES is shown in Fig. 4. The left column plots in Fig. 4 illustrate that a continuous supply of hydrogen at a rate of 2 kg/s fills the HES to capacity in 9 hours. The right column in Fig. 4 shows the HES behavior when charged or discharged with hydrogen at a rate between 0 to 2 kg/s. The positive value for the flow rate indicates charging, while the negative value indicates discharging.

2.1.3. Polymer Electrolyte Membrane

PEM water electrolysis is regarded as one of the most promising mechanisms for high purity and efficient hydrogen production from renewable energy sources, emitting only oxygen as a byproduct. Furthermore, the hydrogen and oxygen generated can be utilized directly in fuel cells and other industrial uses. PEM electrolysis converts water to hydrogen using only electricity and consequently has lower efficiency than HTSE. According to [32], the PEM subsystem needs 50.2 kWh_e per kg of H_2 produced, making the PEM system 66% efficient.

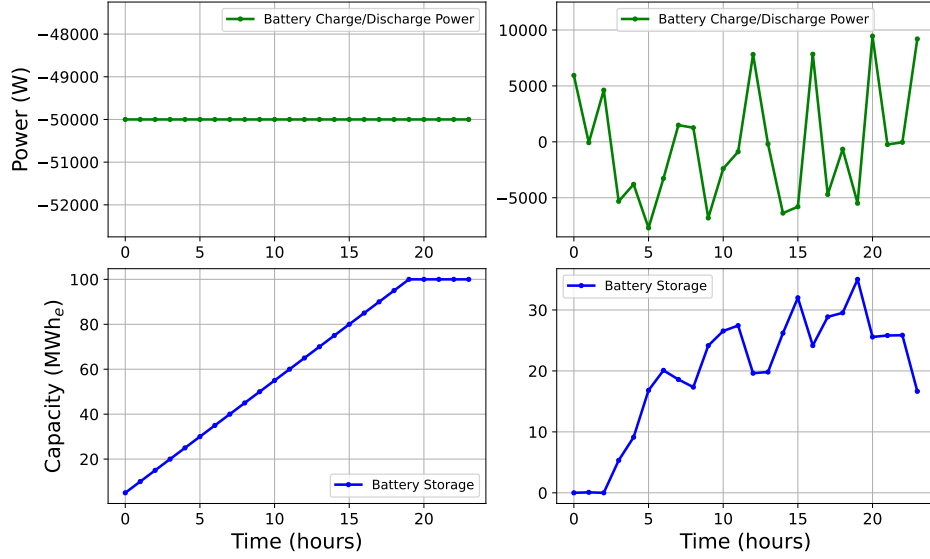


Figure 5: BES charging/discharging behavior for 24 hours.

Considering these factors, the linear relationship in (1) is used to model the PEM.

$$H_p^{\text{pem}} = K_e^{\text{pem}} P_e \quad (1)$$

Here, H_p^{pem} is the hydrogen-production rate from PEM in kg/s, P_e is the electric power input in MW_e , and K_e^{pem} is the corresponding coefficient according to the model efficiency information.

2.2. Modelica Model

Modelica is an equation-based object-oriented modeling language for large, complex, and heterogeneous physical systems. It is used to simulate continuous and discrete-event physical systems. The battery energy storage (BES) subsystem is programmed in Modelica and exported as an FMU using the Open Modelica tool [33]. This model is from Idaho National Laboratory's open-source hybrid model repository [34]. The BES is designed with an efficiency of 95% and a capacity of 100 MWh_e . It uses a power setpoint as an input variable for charging and discharging.

Fig. 5 depicts the sampled behavior of BES when charge and discharge signals are dispatched to it throughout the day. The charging is represented by a negative value, while a positive value represents discharging. When the input to the model attempts to deplete the BES when it is already empty, its state of charge remains at zero. When it attempts to replenish additional energy when the BES is already full, it will remain at its maximum capacity.

2.3. Simulink Models

In this work, solid oxide electrolyzer cells (SOEC) were modeled for the high-temperature steam electrolysis (HTSE) process. The solid oxide cell (SOC) is also capable of operating in reverse mode, wherein it utilizes hydrogen as a fuel source to generate electrical energy. A Simulink solid oxide fuel cell (SOFC) model was also developed for the NR-IES environment. To facilitate the integration of these Simulink models into the proposed

co-simulation framework, it was necessary to develop a standalone FMU for them. This was achieved by using FMI Kit, an external tool developed for Simulink that supports FMU export [35].

2.3.1. High Temperature Steam Electrolysis

The steam generated by the thermal energy from NPPS is directly utilized by the high-temperature steam electrolysis (HTSE) for H₂ production. HTSE improves its efficiency by splitting steam into hydrogen and oxygen in solid-oxide electrolyzer cells (SOECs). Compared to traditional water electrolysis, SOEC splits high temperature (800–1000°C) steam, which requires less electricity. Increased efficiency and use of inexpensive thermal energy, along with reduced electricity requirement, lowers the overall H₂ production costs. A Simulink SOEC model detailed in [36] has been used in this work.

In this model, the molar rates of hydrogen production during electrolysis given by (2) can be predicted independently using the measured stack current, I , and the no. of cells in the stack, N_{cells} ,

$$\Delta\dot{N}_{H_2} = \frac{I}{2F}N_{\text{cells}} \quad (2)$$

Here, $\Delta\dot{N}_{H_2}$ is the hydrogen production rate from SOEC and F is Faraday’s constant. The comprehensive model design, mathematical equations, parameter values, and validation are outlined in [36].

2.3.2. Solid Oxide Fuel Cell

The SOFC model was developed using the partial pressure equations for H₂, O₂, and H₂O gases. Based on the partial pressure calculations detailed in [36], the SOFC overall stack output voltage was calculated using (3),

$$V_{fc} = N_0 \left(E_0 + \frac{RT}{2F} \left(\ln \frac{P_{H_2} P_{O_2}^{0.5}}{P_{H_2O}} \right) \right) - rI_{fc} \quad (3)$$

where, I_{fc} the stack load current, q_{H_2} is the fuel/hydrogen flow rate, and q_{O_2} is the oxygen flow rate. K_{H_2} , K_{O_2} , and K_{H_2O} are the molar valve constants for hydrogen, oxygen, and water, respectively. N_0 is the number of cells in a stack, E_0 is the standard reversible cell potential, R is the universal gas constant, T is the temperature of the stack, F is the Faraday’s constant, and r is the stack’s ohmic loss.

The total power output from the fuel cell is the product of the stack voltage and current multiplied by the total number of stacks considered for the fuel cell subsystem in the NR-IES. All the parameters used in modeling the SOFC stack, its design, and its validation are described in [36].

2.4. Data Sources

2.4.1. Electricity Prices and Wind Power

Electricity pricing and wind generation power utilized in operational simulations are based on real-world locational marginal pricing (LMP) and power generation data from Pennsylvania-New Jersey-Maryland (PJM) Inter-

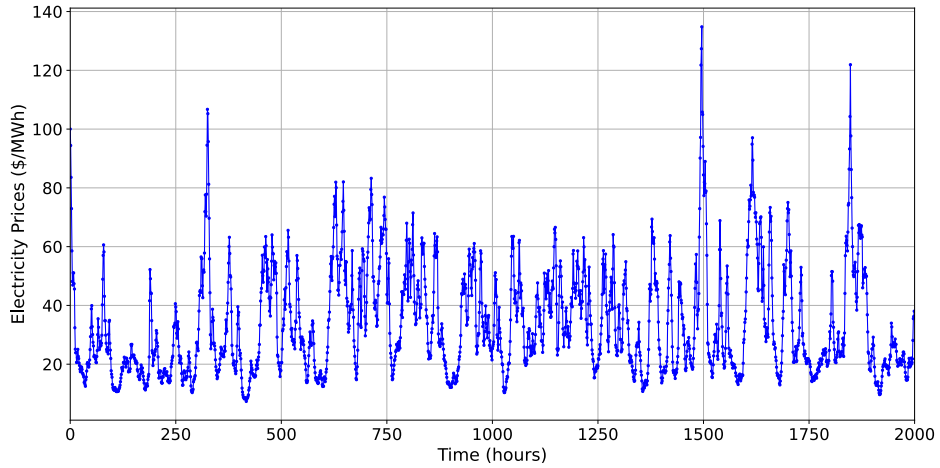


Figure 6: Historical hourly day-ahead electricity data for the pricing nodes DAVISBES and PERRY_FE.

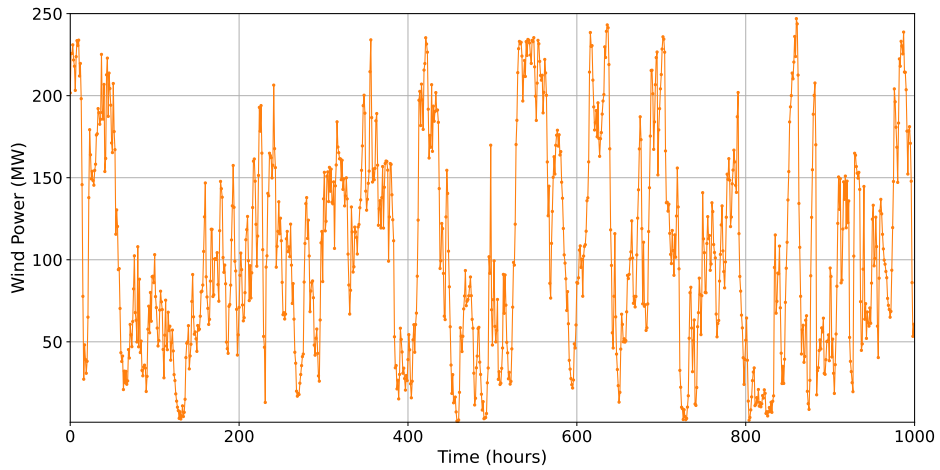


Figure 7: Wind power data.

connection [37]. Since PJM provides data for multiple pricing nodes, DAVISBES and PERRY_FE were selected for electricity prices, which are Ohio-specific nuclear power plant nodes. Fig. 6 shows historical hourly electricity market pricing data for the aforementioned pricing nodes for the last 2000 hours in the year 2020. Fig. 7 shows the variability in wind power generation over a period of 1000 hours. These data were incorporated in the NR-IES environment as uncontrollable states to provide stochastic input. The data is scaled in accordance with other system components to support simulations within the proposed framework.

2.4.2. Hydrogen Prices

The study in [38] includes the hydrogen demand for a researched region as well as natural gas price forecasts for high, low, and medium levels. For the simulations in this paper, various combinations of hydrogen production rates and hydrogen prices under the medium natural gas price scenario were used. For each simulation case of hydrogen production rate and price, the hydrogen price and demand were kept constant, and it was ensured that the system met the fixed hydrogen demand every hour.

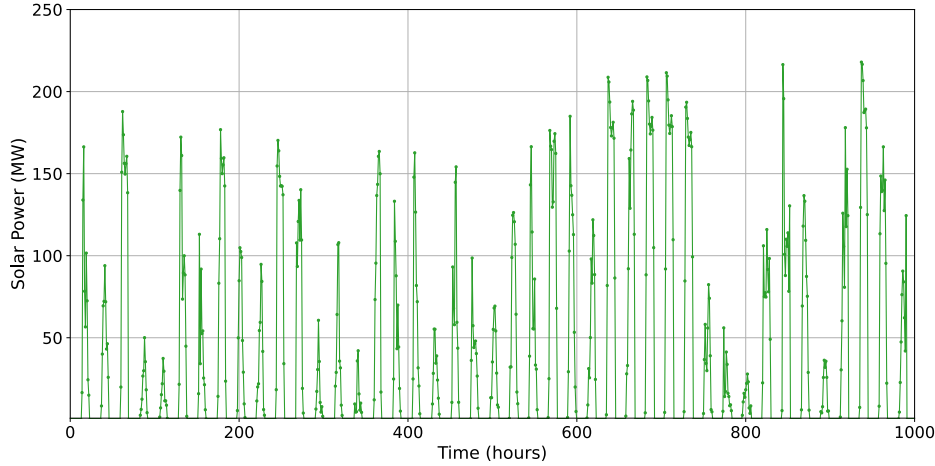


Figure 8: Solar power data.

2.4.3. Solar Power

Solar power data for this work was generated from a solar field model designed using PVLlib [39]. The weather data, such as solar irradiance, temperature, etc., required as input into the solar field model was obtained from the typical meteorological year (TMY) database maintained by the National Renewable Energy Laboratory (NREL) [40]. For the TMY dataset, the region around the Ohio-specific nuclear power plant was selected. The generated solar power data was pre-processed to fit the time scale of the electricity pricing and wind power data. Fig. 8 shows the variations in the solar power data over a period of 1000 hours.

2.5. NR-IES Framework

All these subsystems developed in diverse platforms were integrated via the FMI interface, and a tightly coupled NR-IES framework was formed. Fig. 1 represents the NR-IES framework overview that was developed and simulated to investigate energy dispatching decisions to improve the IES's performance. The NR-IES framework is adaptable to episodes of varying lengths and is straightforward to implement. The analyses in this study are limited to a 1-day (24-hour) control time frame or episode. In the proposed design, the combination of NPPS and renewable energy were considered as energy inputs. The main mechanism of the NR-IES for producing heat is the NPPS. This work makes the assumption that the primary heat generation system is a modular reactor with a nominal capacity of 600 MW_{th} and is treated as a constant thermal energy source [41]. This energy can be converted to either electricity or hydrogen, or it can be retained for future use as thermal, electric, and hydrogen (chemical) energy. Depending on varying electricity market prices, the amount of energy to be sold, stored, or converted was selected to maximize the overall revenue. In this framework, surplus thermal power from NPPS may be immediately directed into the HTSE system to produce H₂ or converted to electricity via the nuclear plant secondary system (NPSS), generally referred to as a turbine island. A linear relationship was considered for thermal power to electricity conversion with an efficiency of 33% [42]. PEM may also be employed with power from wind and solar renewable sources included in the energy park. The system participates in the electricity and hydrogen markets and incorporates thermal energy

storage (TES), hydrogen energy storage (HES), and battery energy storage (BES) solutions to augment flexibility. When there is a sudden surge in electricity prices, the HES system supplies stored hydrogen to the fuel cell to produce grid-compatible electricity. Based on [38], constant hydrogen demand and price configurations have been considered in this work. For intermediary electricity conversion, a 3-phase bidirectional inverter and rectifier with an efficiency of 95% was used to convert AC to DC power and vice-versa. The DRL agent decides the usage of the mentioned storage systems to maximize the revenue of the overall system. For example, if the electrical energy production is high and electricity prices are low, surplus thermal and electrical energy can be stored in the TES and BES, respectively, and used whenever the pricing signals are favorable to attain greater flexibility and revenue. In this scenario, the DRL agent will recommend that the production of hydrogen be increased for additional revenue. This work focuses on generating more revenue without the consideration of capital costs for hydrogen systems, storage systems, or power converters.

3. Power Dispatching Strategy Optimization in NR-IES Using DRL

3.1. NR-IES Optimization Problem Formulation

In this section, the NR-IES optimization problem is described as an MDP (Markov decision process). The objective of the problem is to find the optimal dispatching strategy of the energy conversion and energy storage systems so that the NR-IES can maximize daily revenue and ensure stability. An agent is defined using DRL, which utilizes artificial neural networks with a reinforcement learning framework that enables it to learn to meet its goals. The problem modeled using MDP is typically expressed as a tuple (S, A, P, R, π) , which includes: state-space (S), action space (A), state transition probability (P), reward (R), and the policy of the agent (π).

The state space can be expressed as a vector, $S = [S_0, S_1, S_2, S_3, S_4, S_5]$. Given the state S , the agent will take an action which is given by, $A = [A_0, A_1, A_2, A_3, A_4]$. The states listed in Table 1 can be updated and controlled at each time step with the control actions detailed in Table 2.

Given an action (A), the environment has a transition probability, $P(S'|S, A)$ of mapping the control action (A) to the associated next state value (S') and reward value (R) as shown in Fig. 9. The reward (R) of the MDP

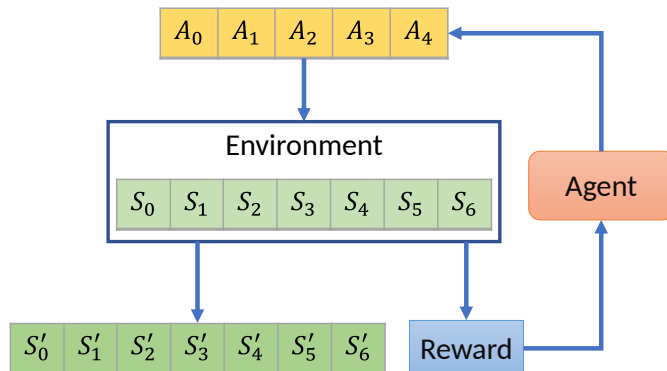


Figure 9: The agent-environment interaction in reinforcement learning.

Table 1: Proposed States for Environment

| States | |
|--------|---------------------------------------|
| S_0 | Thermal power from NPPS (MW_{th}) |
| S_1 | Wind power (MW_e) |
| S_2 | Solar power (MW_e) |
| S_3 | Electricity price ($\$/MW_e$) |
| S_4 | Battery energy storage (MWh_e) |
| S_5 | Thermal energy storage (MWh_{th}) |
| S_6 | Hydrogen energy storage (kg) |

Table 2: Proposed actions for Environment

| Actions | |
|---------|---|
| A_0 | Thermal power to TES (MW_{th}) |
| A_1 | Thermal and electric power to HTSE (MW_{th} and MW_e) |
| A_2 | Electric power to PEM (MW_e) |
| A_3 | Electric power to BES (MW_e) |
| A_4 | Hydrogen from HES to fuel cell (kg) |

problem is its cumulative value over time. Optimal energy dispatch aims to increase IES revenue while maintaining system stability. As a result, the problem of maximizing the objective function becomes a problem of maximizing the reward function. The policy set represents the mapping relation from the state space to the action space. Based on the agent policy, an action (A), is chosen to update the state space from S to S' . The MDP aims to determine the policy set that maximizes expected return. The total reward at time step, t can be modeled as (4),

$$r(t) = 0.001 * [Revenue(t) - \sum c_i(t)]. \quad (4)$$

To regulate the DRL agent’s behavior, revenues earned from selling electricity and hydrogen are treated as positive rewards in (4), while the costs of penalties, $c_i(t)$ are depicted as negative rewards. In (4), α_i is an arbitrary constant (weighing parameter) that controls the importance of costs and penalties. For example, when calculating penalties for out-of-bound storage, $f_c^{storage}$ in (5), the value considered for α_i is greater compared to the value considered when calculating penalties for f_c^{bes} , f_c^{tes} , f_c^{hes} in (6), (7) and (8) respectively, which are within its limits. Additional reward conditions can be included to regulate the DRL agent’s behavior. The potential penalty components are modeled as follows:

$$c_1(t) = \alpha_1 f_c^{storage}(update(t), feasiblerate(t)) \quad (5)$$

$$c_2(t) = \alpha_2 f_c^{bes}(STGE_{bes}(t), STGE_{bes}^{low}, STGE_{bes}^{high}) \quad (6)$$

$$c_3(t) = \alpha_3 f_c^{tes}(STGE_{tes}(t), STGE_{tes}^{low}, STGE_{tes}^{high}) \quad (7)$$

$$c_4(t) = \alpha_4 f_c^{hes}(STGE_{hes}(t), STGE_{hes}^{low}, STGE_{hes}^{high}) \quad (8)$$

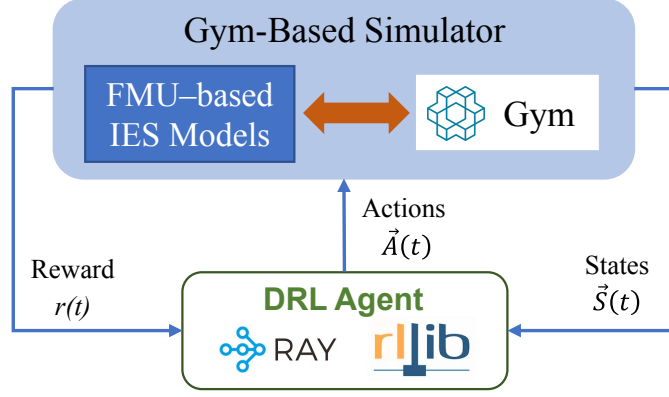


Figure 10: DRL framework based on OpenAI Gym and Ray/RLlib.

$$c_5(t) = \alpha_5 f_c^{\text{hydrogen}}(\text{hydrogen}(t)) \quad (9)$$

$$c_6(t) = \alpha_6 f_c^{\text{electricity}}(\text{electricity}(t)) \quad (10)$$

In (5), the function f_c^{storage} calculates the absolute difference between the update action for the storage and feasible charging and discharging rate of the storage at the time, t . $STGE_{\text{bes}}(t)$, $STGE_{\text{tes}}(t)$, $STGE_{\text{hes}}(t)$ in (6), (7) and (8) respectively, are the level of energy in BES, TES and HES at t . Each storage system has its own cost function within a specific preferable operating range: $[STGE^{\text{low}}, STGE^{\text{high}}]$. A potential functional format for cost functions, f_c^{bes} , f_c^{tes} , f_c^{hes} in (6), (7) and (8), respectively, is regarded as an absolute difference between current storage level, $STGE$ and $[STGE^{\text{low}}$ or $STGE^{\text{high}}]$. The cost functions, f_c^{hydrogen} and $f_c^{\text{electricity}}$ in (9) and (10) ensure that hydrogen and electricity are never negative at any time step, t .

3.2. DRL Framework

A promising computational framework based on OpenAI Gym [43] and Ray/RLlib [44] has been developed to facilitate the simulation and training process, as shown in Fig. 10. The operations and interactions between the various NR-IES subsystem components in Fig. 1 were simulated using FMU-based models and can be incorporated into the OpenAI Gym environment. According to the suggested states, actions, and reward functions from the MDP model presented in the preceding section, a custom Gym-based NR-IES simulator was constructed. The Gym-based NR-IES simulator was integrated into Ray/RLlib, as illustrated in Fig. 10. This computational architecture allows for flexible and fast simulations and the implementation, training, and evaluation of various DRL algorithms for NR-IES power flow dispatch.

3.3. DRL Algorithm

Reinforcement learning (RL), a machine learning approach influenced by human behavior, is concerned with how an agent should operate in a stochastic environment to maximize the cumulative reward. DRL is a technique that effectively integrates RL's decision-making capacity with deep learning's perception. It uses a deep neural

network (DNN) to represent the value function, which provides target values and RL to generate the reward equal to the estimated value. The DNN’s parameters are adjusted regularly until the discrepancy between the target and estimated values converges.

PPO is a novel on-policy algorithm, which means that its value function is derived from observations made by the current policy as it explores the environment. On the contrary, off-policy algorithms can benefit from observations during previous policies’ environmental investigations. The choice between off-policy and on-policy learning is frequently a trade-off between stability and data efficiency. As a result, PPO is more stable compared to off-policy algorithms despite the fact that it requires more data during the training phase and, therefore, is slower. In [45], the DRL algorithms, deep deterministic policy gradient (DDPG), deep q-network (DQN), and proximal policy optimization (PPO) are compared against a traditional control technique, mixed integer linear program (MILP), to illustrate DRL’s superiority for regulating IES. PPO performed better than other approaches, displaying more consistent performance and higher generalization abilities. Furthermore, in a previous iteration of this work [17], PPO demonstrated more stable performance in comparison to other popular DRL algorithms. Hence, PPO is a superior DRL algorithm for optimizing power dispatching strategies in interconnected energy systems [17], [46] and, therefore, was utilized in this study as the DRL algorithm of choice to optimize the NR-IES.

4. Results and Discussion

4.1. Training

The primary configuration parameters used in the proposed NR-IES simulator framework are shown in Table 3. The constraints used for the HTSE, PEM, and fuel cell subsystems are also shown in Table 3. Lower limit values for HTSE and PEM are kept low because hard limits are not well known, and exact limits have no significant effect on

Table 3: Primary Configurations in NR-IES Simulation

| | |
|---|-----------|
| Total thermal power from NPPS (MW_{th}) | 600 |
| Efficiency of thermal energy to electricity in NPSS (%) | 33 |
| Limits of electric power for HTSE (MW_e) | [0.1, 60] |
| Limits of thermal power for HTSE (MW_{th}) | [0, 16.4] |
| Limits of electric power for PEM (MW_e) | [1, 200] |
| HES capacity (kg) | 72000 |
| TES capacity (MWh_{th}) | 10000 |
| BES capacity (MWh_e) | 100 |
| TES maximum charging/discharging power (MW_{th}) | 500 |
| HES maximum discharging/charging rate (kg/s) | 10 |
| BES maximum charging power (MW_e) | 20 |
| TES initial SOC (%) | 10 |
| HES initial SOC (%) | 10 |
| BES initial SOC (%) | 30 |
| Hydrogen from HES to fuel cell (kg/hr) | [1, 2000] |
| Hydrogen market demand (kg/hr) | 1250 |
| Hydrogen price (\$/kg) [38] | 2.675 |

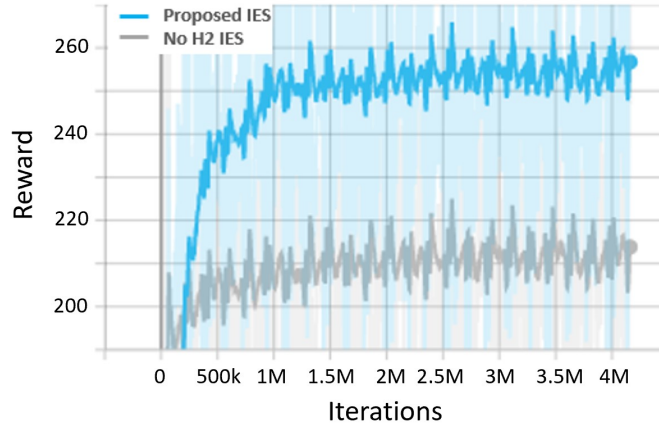


Figure 11: Mean reward during DRL training for scenarios with and without hydrogen production, storage, and utilization.

simulation results. For the storage subsystems, the DRL agent was heavily penalized while training if the storage capacity dropped below 30% for the BES and 10% for the HES and TES. Additionally, as a base case, a separate NR-IES framework is developed and simulated that does not include hydrogen production or storage subsystems and instead focuses solely on the generation of electricity for the grid.

The training results of both cases are shown in Fig. 11. The blue line shows the mean reward for the NR-IES simulator with both hydrogen and electricity production over 4 million training iterations. The grey line shows the mean reward for the NR-IES simulator with only electricity production. The environment that contains hydrogen performs better with a significantly greater reward gain.

4.2. Testing

After testing the trained agent with and without hydrogen, the reward and revenue over 120 days are shown in Fig. 12. As anticipated, the revenue trend pattern depicted in Fig. 12b strongly aligns with the reward trend

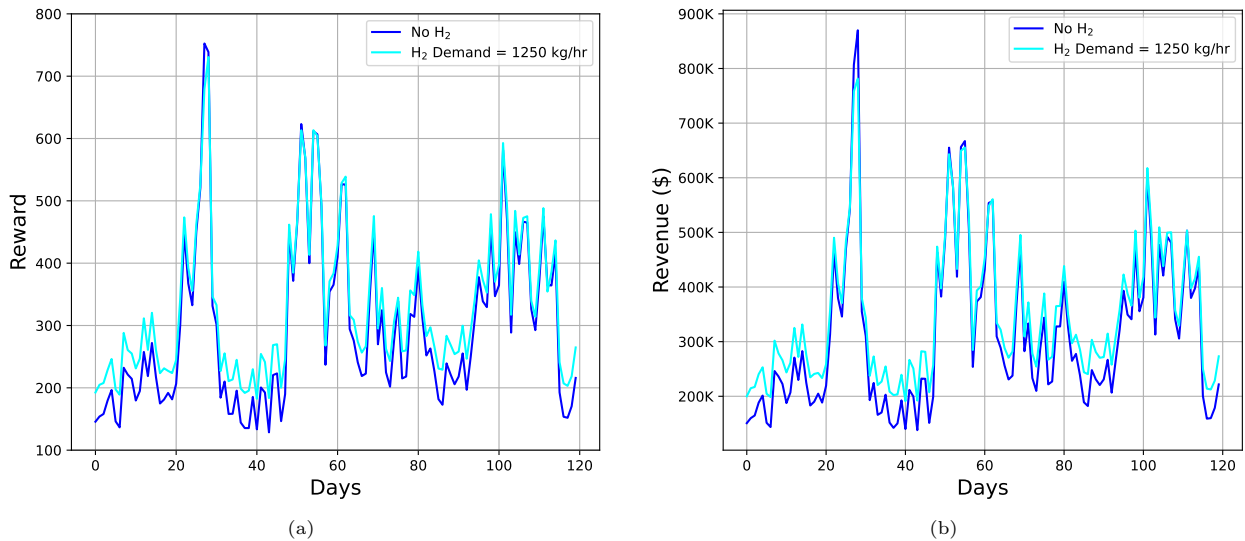


Figure 12: The comparison between with and without hydrogen environments showing (a) the reward over 120 days, and (b) the revenue generated over 120 days.

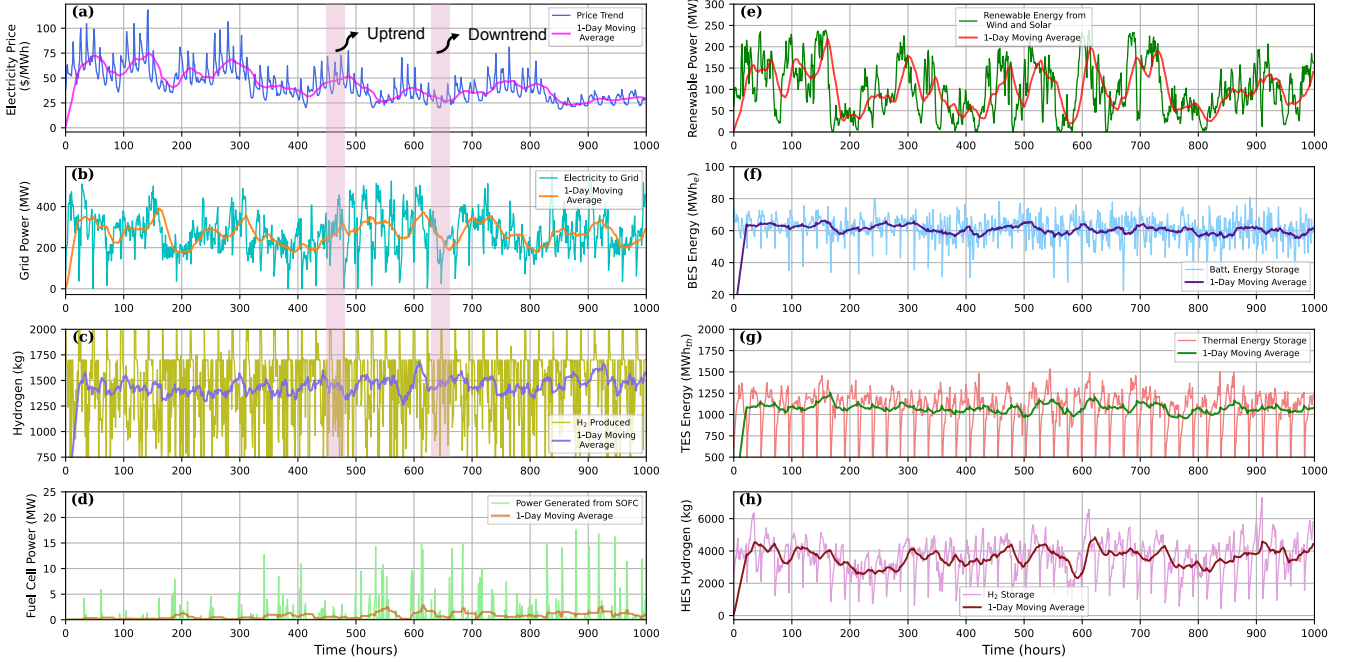


Figure 13: Electricity price and renewable power data fed to the NR-IES during testing along with selected subsystem states controlled by the trained DRL agent over a period of 1000 hours.

in Fig. 12a. From Fig. 12a, it is clear that, at most times, the environment with hydrogen production has more rewards than the environment without hydrogen. The revenue for the IES without hydrogen can be calculated as, $electricity\ price\ (\$/MW_e) \times electricity\ to\ grid\ (MW_e)$. Revenue for the environment with hydrogen is calculated as, $hydrogen\ price\ (\$/kg) \times hydrogen\ sell\ to\ market\ (kg) + electricity\ price\ (\$/MW_e) \times electricity\ to\ grid\ (MW_e)$. The revenue calculation occurs at each time step of an episode, where one episode is a day with a time step of one hour. Over 120 days (2880 hours) of testing, the revenue for each hour is produced. The optimization objective is set to maximize revenue over a 24-hour period. The total revenue per day in Fig. 12b is calculated by summing up hourly revenue for 24 hours. It is noteworthy that there are three instances in which the environment without hydrogen gives more revenue than the environment with hydrogen. Each of those instances represents extreme conditions in which the daily revenue is greater than \$600,000. However, considering a longer period, the total revenue from the IES with hydrogen is more than the revenue without hydrogen.

Fig. 13 shows the varying trends in selected subsystems and was generated while testing the trained DRL agent on the NR-IES environment with a constant H₂ demand of 1250 kg/hr. The graphs are smoothed with a 1-day moving average line so that the general trend for each graph can be observed. Fig. 13a and 13e show the stochastic electricity pricing and renewable energy data, respectively, fed to the NR-IES environment as exogenous inputs. As previously stated, the input of a constant 600 MWh_{th} thermal energy was also taken into account since the thermal power output of nuclear reactors rarely fluctuates. The renewable energy data in Fig. 13e is a sum of the wind energy and solar energy data shown in Fig. 7 and Fig. 8, respectively. Based on the stochastic pricing and renewable energy data input, the trained DRL agent would take action to maximize the revenue of the overall

integrated energy system by flexibly varying the production of electricity and hydrogen. Fig. 13b shows the power sent to the grid by the DRL agent. It is evident from Fig. 13b that, unlike a conventional NPP, the power sent to the grid aligns with the value of electricity price, demonstrating the flexibility of the proposed NR-IES. Fig. 13c shows the trend in H₂ production by the HTSE and PEM systems, which also show variations based on the inputs. Fig. 13f, 13g, and 13h show the storage capacity patterns in the BES, TES, and HES, respectively. These storage systems increase the flexibility of the NR-IES by storing and releasing electrical power, thermal power, and hydrogen in an effort to maximize revenue.

Although several factors could influence the actions taken by the DRL agent, two opposite trends are highlighted in Fig. 13a, 13b, and 13c to demonstrate the efficacy of the DRL agent’s decisions based on the concept of transactive energy. In the highlighted downtrend, the price of electricity is decreasing. In response, the DRL agent decides to reduce the amount of power sent to the grid and increase the production of hydrogen. As previously stated, H₂ production increases, and less power is transmitted to the grid at low grid prices. Conversely, the highlighted uptrend indicates rising electricity prices; thus, the DRL agent sends more power to the grid and reduces H₂ production. Again, this decision is anticipated, as increasing grid prices necessitates sending more power to the grid and ramping down H₂ production. As previously mentioned, the DRL agent’s decision may not always correspond with the trends emphasized in Fig. 13. In addition, the fuel cell subsystem output shown in Fig. 13d was negligible since the fuel cell subsystem should only be utilized when there is ample H₂ stored and grid prices are extremely high.

Fig. 14 represents a comparison of the cumulative revenue over 120 days. Three scenarios have been considered with different hydrogen demands. As seen in Fig. 14, the curve corresponding to a hydrogen demand of 1250 kg/hr is consistently higher than the curve corresponding to no hydrogen demand. These results are tabulated in Table 4.

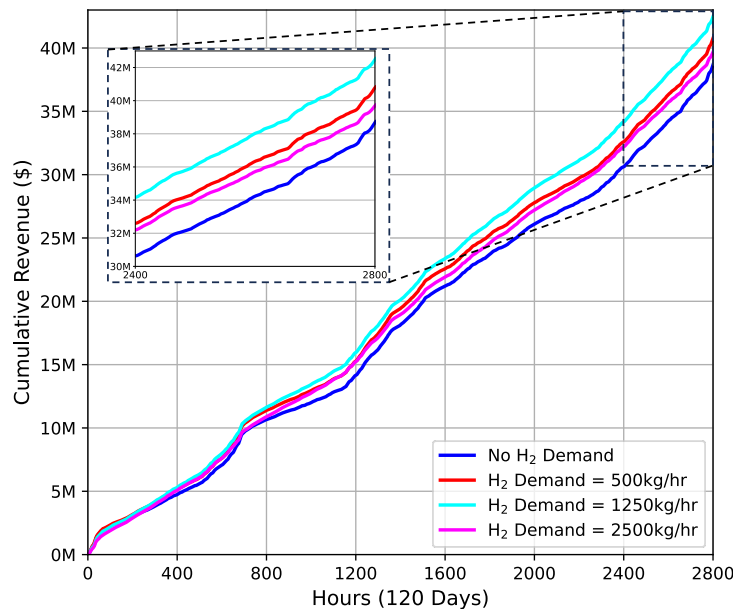


Figure 14: Cumulative revenue: with and without hydrogen IES.

Table 4: Total Reward and Revenue Over 120 Days for Various Hydrogen Demand Cases

| H₂ Demand (kg/hr) | Reward | Revenue (\$) | Increase in Revenue (%) |
|-------------------------------------|---------------|---------------------|--------------------------------|
| No H ₂ | 39959 | 40049037 | 0 |
| 500 | 40589 | 42167373 | 5.3 |
| 1250 | 43802 | 43920975 | 9.7 |
| 2500 | 39384 | 41003194 | 2.4 |

Analysis of both Fig. 14 and Table 4 reveals that environments with hydrogen demands of 500 kg/hr, 1250 kg/hr, and 2500 kg/hr have increased revenues of 5.3%, 9.7%, and 2.4% greater, respectively, compared to the baseline environment without hydrogen. The amount of hydrogen demand clearly influences revenue maximization. Low hydrogen demand limits the environment’s ability to generate revenue from hydrogen when electricity prices are low. High hydrogen demand forces the environment to meet demand even in the face of high electricity prices, reducing the overall revenue generation capability. However, all considered scenarios provide greater revenue than the scenario without hydrogen.

4.3. Practical Considerations

Capital cost analyses of constructing such hydrogen production plants confirm their practicability. Based on the study in [47], the total capital investment of installing a large scale HTSE system is \$703/kW. The HTSE system configured for this simulation has a rated power of 76.4 MW, which translates to an investment of approximately \$53.7M. From the simulation results in this paper, an additional revenue of approximately \$4M over 120 days can be generated from hydrogen. With this additional revenue, such capital costs would be recuperated in less than four years’ time.

While the implementation of TES in this work may be somewhat simplistic, there are several studies that confirm its use with NPPs to enhance their flexibility [48], [49], [50]. In order to optimize the utilization of a TES within a nuclear energy park, some adjustments can be implemented. For example, the stored thermal power could potentially be utilized directly by the low pressure turbine system in the nuclear plant secondary system. However, this process will yield a low level of efficiency. An additional use could involve the utilization of supplementary heaters to reheat the steam from the TES and pass it directly to the high pressure turbine systems in the secondary system to generate electricity. Furthermore, the thermal energy from TES could be used for several other applications, including desalination or purification processes [51].

5. Conclusion and Future Work

This research proposes a modular co-simulation framework for a hydrogen-based nuclear-renewable integrated energy system. The proposed IES combines hydrogen production and storage systems with nuclear and renewable energy sources. An FMI/FMU-based simulator connected with OpenAI Gym and Ray/RLlib was created for the

proposed framework operations, providing a fast and flexible computational environment for DRL-based optimization studies. The modular nature of the proposed framework enhances its overall adaptability and scalability. The PPO algorithm was used to optimize the power dispatching decisions in the IES to augment the flexibility of the nuclear energy park based on grid demand and maximize the overall revenue of the proposed NR-IES. Additionally, the DRL-based optimization framework circumvents the need for a complex mathematical optimization function formulation for the IES. The results have also demonstrated that, in comparison to non-hydrogen IES, the proposed hydrogen-based IES framework achieved approx. 10% revenue gain over 120 days. Overall, the proposed framework can co-simulate several subsystem models within an integrated energy system with a high degree of fidelity while maintaining adaptability and efficiency.

For future work, a pricing model based on a supply-demand curve when considering variable hydrogen demand throughout the day will be explored. High-fidelity models, such as physics-based HTSE and PEM models, will be employed to assist DRL training. An in-depth analysis of each subsystem will be performed to garner insight as to how each component affects revenue maximization. The proposed methodology will explore DRL performance for episodes with longer time horizons, such as one week, one month, etc., which presents more uncertainty to handle. Finally, software representations of physical elements can be substituted for real-time hardware-in-the-loop co-simulations.

Acknowledgments

This work was supported by a grant from the US Department of Energy under prime contract #DE-AC07-05ID14517 and subcontract #236035.

References

- [1] M. M. Rahman, Environmental degradation: The role of electricity consumption, economic growth and globalisation, *Journal of Environmental Management* 253 (2020) 109742.
- [2] J. Nowotny, J. Dodson, S. Fiechter, T. M. Gür, B. Kennedy, W. Macyk, T. Bak, W. Sigmund, M. Yamawaki, K. A. Rahman, Towards global sustainability: Education on environmentally clean energy technologies, *Renewable and Sustainable Energy Reviews* 81 (2018) 2541–2551.
- [3] R. Právělie, G. Bandoc, Nuclear energy: Between global electricity demand, worldwide decarbonisation imperativeness, and planetary environmental implications, *Journal of Environmental Management* 209 (2018) 81–92.
- [4] S. Adams, A. O. Acheampong, Reducing carbon emissions: the role of renewable energy and democracy, *Journal of Cleaner Production* 240 (2019) 118245.

- [5] S. M. Bragg-Sitton, R. Boardman, C. Rabiti, J. O'Brien, Reimagining future energy systems: Overview of the us program to maximize energy utilization via integrated nuclear-renewable energy systems, *International Journal of Energy Research* 44 (10) (2020) 8156–8169.
- [6] M. F. Ruth, O. R. Zinaman, M. Antkowiak, R. D. Boardman, R. S. Cherry, M. D. Bazilian, Nuclear-renewable hybrid energy systems: Opportunities, interconnections, and needs, *Energy Conversion and Management* 78 (2014) 684–694.
- [7] S. Suman, Hybrid nuclear-renewable energy systems: A review, *Journal of Cleaner Production* 181 (2018) 166–177.
- [8] H. A. Gabbar, M. I. Adham, M. R. Abdussami, Analysis of nuclear-renewable hybrid energy system for marine ships, *Energy Reports* 7 (2021) 2398–2417.
- [9] B. E. Türkay, A. Y. Telli, Economic analysis of standalone and grid connected hybrid energy systems, *Renewable Energy* 36 (7) (2011) 1931–1943.
- [10] A. Hajimiragha, C. Canizares, M. Fowler, M. Geidl, G. Andersson, Optimal energy flow of integrated energy systems with hydrogen economy considerations, in: *iREP Symposium on Bulk Power System Dynamics and Control*, 2007, pp. 1–11.
- [11] T. Capurso, M. Stefanizzi, M. Torresi, S. Camporeale, Perspective of the role of hydrogen in the 21st century energy transition, *Energy Conversion and Management* 251 (2022) 114898.
- [12] J. Liu, Z. Xu, J. Wu, K. Liu, X. Guan, Optimal planning of distributed hydrogen-based multi-energy systems, *Applied Energy* 281 (2021) 116107.
- [13] G. Wu, T. Li, W. Xu, Y. Xiang, Y. Su, J. Liu, F. Liu, Chance-constrained energy-reserve co-optimization scheduling of wind-photovoltaic-hydrogen integrated energy systems, *International Journal of Hydrogen Energy*.
- [14] G. Pan, W. Gu, H. Qiu, Y. Lu, S. Zhou, Z. Wu, Bi-level mixed-integer planning for electricity-hydrogen integrated energy system considering levelized cost of hydrogen, *Applied Energy* 270 (2020) 115176.
- [15] P. Ge, Q. Hu, Q. Wu, X. Dou, Z. Wu, Y. Ding, Increasing operational flexibility of integrated energy systems by introducing power to hydrogen, *IET Renewable Power Generation* 14 (3) (2020) 372–380.
- [16] EERE, Hydrogen Shot, <https://www.energy.gov/eere/fuelcells/hydrogen-shot>, accessed: 2023-07-03.
- [17] Z. Yi, Y. Luo, T. Westover, S. Katikaneni, B. Ponkiya, S. Sah, S. Mahmud, D. Raker, A. Javaid, M. J. Heben, et al., Deep reinforcement learning based optimization for a tightly coupled nuclear renewable integrated energy system, *Applied Energy* 328 (2022) 120113.

- [18] D. S. Schiera, L. Barbierato, A. Lanzini, R. Borchiellini, E. Pons, E. Bompard, E. Patti, E. Macii, L. Bottaccioli, A distributed multimodel platform to cosimulate multienergy systems in smart buildings, *IEEE Transactions on Industry Applications* 57 (5) (2021) 4428–4440.
- [19] T. Blockwitz, M. Otter, J. Akesson, M. Arnold, C. Clauss, H. Elmqvist, M. Friedrich, A. Junghanns, J. Mauss, D. Neumerkel, et al., Functional mockup interface 2.0: The standard for tool independent exchange of simulation models, in: *Proceedings of the 9th International MODELICA Conference, 2012*, pp. 173–184.
- [20] A. Bischi, L. Taccari, E. Martelli, E. Amaldi, G. Manzolini, P. Silva, S. Campanari, E. Macchi, A detailed MILP optimization model for combined cooling, heat and power system operation planning, *Energy* 74 (2014) 12–26.
- [21] K. Anoune, A. Laknizi, M. Bouya, A. Astito, A. B. Abdellah, Sizing a PV-wind based hybrid system using deterministic approach, *Energy Conversion and Management* 169 (2018) 137–148.
- [22] F. Vitale, N. Rispoli, M. Sorrentino, M. Rosen, C. Pianese, On the use of dynamic programming for optimal energy management of grid-connected reversible solid oxide cell-based renewable microgrids, *Energy* 225 (2021) 120304.
- [23] A. Stoppato, G. Cavazzini, G. Ardizzon, A. Rossetti, A PSO (particle swarm optimization)-based model for the optimal management of a small pv (photovoltaic)-pump hydro energy storage in a rural dry area, *Energy* 76 (2014) 168–174.
- [24] E. Mocanu, D. C. Mocanu, P. H. Nguyen, A. Liotta, M. E. Webber, M. Gibescu, J. G. Slootweg, On-line building energy optimization using deep reinforcement learning, *IEEE Transactions on Smart Grid* 10 (4) (2018) 3698–3708.
- [25] H. Hua, Y. Qin, C. Hao, J. Cao, Optimal energy management strategies for energy internet via deep reinforcement learning approach, *Applied Energy* 239 (2019) 598–609.
- [26] S. Mahmud, S. Sah, B. Ponkiya, S. Katikaneni, D. Raker, M. Heben, R. Khanna, A. Javaid, Z. Yi, T. Westover, et al., A transactive energy framework for hydrogen production with economically viable nuclear power, in: *2022 IEEE/PES transmission and distribution conference and exposition (T&D), IEEE, 2022*, pp. 1–5.
- [27] B. Zhang, W. Hu, D. Cao, Q. Huang, Z. Chen, F. Blaabjerg, Deep reinforcement learning-based approach for optimizing energy conversion in integrated electrical and heating system with renewable energy, *Energy Conversion and Management* 202 (2019) 112199.
- [28] J. Schulman, F. Wolski, P. Dhariwal, A. Radford, O. Klimov, Proximal policy optimization algorithms, *arXiv Prepr. arXiv1707.06347*.

- [29] M. Stifter, E. Widl, F. Andr n, A. Elsheikh, T. Strasser, P. Palensky, Co-simulation of components, controls and power systems based on open source software, in: IEEE Power & Energy Society General Meeting, 2013, pp. 1–5.
- [30] D. Syst mes, FMPy python library, <https://github.com/CATIA-Systems/FMPy>, accessed: 2023-07-03.
- [31] L. I. Hatledal, F. Collonval, H. Zhang, Enabling python driven co-simulation models with pythonfmu, in: Proceedings of the 34th International ECMS-Conference on Modelling and Simulation, 2020, pp. 235–239.
- [32] M. Ruth, D. Cutler, F. Flores-Espino, G. Stark, The economic potential of nuclear-renewable hybrid energy systems producing hydrogen, Tech. Rep. NREL/TP-6A50-66764, National Renewable Energy Lab, Golden, CO (2017).
- [33] P. Fritzson, A. Pop, K. Abdelhak, A. Asghar, B. Bachmann, W. Braun, D. Bouskela, R. Braun, L. Buffoni, F. Casella, et al., The openmodelica integrated environment for modeling, simulation, and model-based development, *Modeling, Identification and Control* 41 (4) (2020) 241–295.
- [34] K. L. Frick, A. Alfonsi, C. Rabiti, Hybrid user manual, <https://www.osti.gov/biblio/1760168>, accessed: 2023-07-03.
- [35] CATIA-Systems, FMI kit for simulink, <https://github.com/CATIA-Systems/FMIKit-Simulink>, accessed: 2023-07-03.
- [36] S. Pandey, S. Mahmud, K. Sravya, J. Ahmad, H. Michael J., W. Victor, Y. Zonggen, W. Tyler, K. Raghav, Modeling of solid oxide -electrolyzer and -fuel cell for nuclear-renewable integrated energy systems, in: 2023 IEEE Power & Energy Society General Meeting (PESGM), IEEE, 2023.
- [37] PJM interconnection website, <https://dataminer2.pjm.com/list>, accessed: 2023-07-03.
- [38] K. L. Frick, P. W. Talbot, D. S. Wendt, R. D. Boardman, C. Rabiti, S. M. Bragg-Sitton, M. Ruth, D. Levie, B. Frew, A. Elgowainy, et al., Evaluation of hydrogen production feasibility for a light water reactor in the midwest, Tech. Rep. INL/EXT-19-55395-Rev000, Idaho National Lab, Idaho Falls, ID (2019).
- [39] W. F. Holmgren, C. W. Hansen, M. A. Mikofski, pvlib python: a python package for modeling solar energy systems, *Journal of Open Source Software* 3 (29) (2018) 884. doi:10.21105/joss.00884.
- [40] National Renewable Energy Laboratory, NSRDB: National solar radiation database, <https://nsrdb.nrel.gov/data-sets/tmy>, accessed: 2023-07-03.
- [41] J. S. Kim, R. D. Boardman, S. M. Bragg-Sitton, Dynamic performance analysis of a high-temperature steam electrolysis plant integrated within nuclear-renewable hybrid energy systems, *Applied Energy* 228 (2018) 2090–2110.

- [42] G. J. Suppes, T. S. Storvick, Chapter 7 - production of electricity, in: Sustainable Nuclear Power, Academic Press, Burlington, MA, 2007, pp. 185–200.
- [43] G. Brockman, V. Cheung, L. Pettersson, J. Schneider, J. Schulman, J. Tang, W. Zaremba, OpenAI gym, arXiv Prepr. arXiv1606.01540.
- [44] E. Liang, R. Liaw, R. Nishihara, P. Moritz, R. Fox, K. Goldberg, J. Gonzalez, M. Jordan, I. Stoica, RLlib: Abstractions for distributed reinforcement learning, in: Proceedings of the 35th International Conference on Machine Learning, Vol. 80 of Proceedings of Machine Learning Research, PMLR, 2018, pp. 3053–3062.
- [45] C. Guo, X. Wang, Y. Zheng, F. Zhang, Real-time optimal energy management of microgrid with uncertainties based on deep reinforcement learning, *Energy* 238 (2022) 121873.
- [46] Y. Zhou, B. Zhang, C. Xu, T. Lan, R. Diao, D. Shi, Z. Wang, W.-J. Lee, A data-driven method for fast ac optimal power flow solutions via deep reinforcement learning, *Journal of Modern Power Systems and Clean Energy* 8 (6) (2020) 1128–1139.
- [47] D. S. Wendt, L. T. Knighton, High temperature steam electrolysis process performance and cost estimates, Tech. Rep. INL/RPT-22-66117-Rev000, Idaho National Lab, Idaho Falls, ID (2022).
- [48] M. Ali, A. K. Alkaabi, J. I. Lee, Cfd simulation of an integrated pcm-based thermal energy storage within a nuclear power plant connected to a grid with constant or variable power demand, *Nuclear Engineering and Design* 394 (2022) 111819.
- [49] A. A. Al Kindi, M. Aunedi, A. M. Pantaleo, G. Strbac, C. N. Markides, Thermo-economic assessment of flexible nuclear power plants in future low-carbon electricity systems: Role of thermal energy storage, *Energy Conversion and Management* 258 (2022) 115484.
- [50] P. Romanos, A. A. Al Kindi, A. M. Pantaleo, C. N. Markides, Flexible nuclear plants with thermal energy storage and secondary power cycles: Virtual power plant integration in a uk energy system case study, *e-Prime-Advances in Electrical Engineering, Electronics and Energy* 2 (2022) 100027.
- [51] V. G. Gude, Energy storage for desalination processes powered by renewable energy and waste heat sources, *Applied energy* 137 (2015) 877–898.